INT. J. NUM. METH. HEAT FLUID FLOW, VOL. 6 NO. 4, 37–46 (1996)

HEATLINE VISUALIZATION IN TURBULENT FLOW

SUKANTA K. DASH
Tata Steel, R & D Division, Jamshedpur 831007, India

ABSTRACT

The concept of a heat function is introduced to visualize the path of heat flow in a buoyancy-driven turbulent flow heated vertical flat plate. The velocities and the temperature field near the vertical plate are predicted numerically, using an algebraic flux model of turbulent heat transport. As an accurate prediction of the turbulent heat flux is required in order to predict the heat function in the flow field, the use of an algebraic flux model for the turbulent heat transport $\overline{\theta u_i}$, is made as compared with a simple eddy diffusivity hypothesis. The algebraic flux expression was closed with a low-*Re*-number-k-ε – $\overline{\theta^2}$ – ε_θ model. The solution of the 4 equation low-*Re*-number-k-ε – $\overline{\theta^2}$ – ε_θ model predicts very well the local Nusselt number along the plate height as well as the velocity and the temperature field near the wall when compared with the experiments. Then the partial differential equation for the heat function is numerically solved to show the true path of heat flow in the buoyancy-driven turbulent flow field near a heated vertical plate.

KEY WORDS Convection Heat transfer Turbulence

NOMENCLATURE

C = Specific heat
g = Acceleration due to gravity
Gr_y = Grasshof number $(g\beta(T_w - T\infty)y^3/\nu^2$
H = Heat function
k = Turbulent kinetic energy
p = Pressure
Pr = Prandtl number
T = Temperature
t = Time
U = Mean velocity in x direction
u = Fluctuating velocity component in x direction
V = Mean velocity in y direction
V_{max} = Maximum local mean velocity in y direction
v = Fluctuating velocity component in y direction
x = Co-ordinate distance in cross-stream direction
y = Co-ordinate distance in streamwise direction
ρ = Density
λ = Thermal conductivity
α = Thermal diffusivity
μ = Viscosity
ν = Kinematic viscosity
β = Coefficient of thermal expansion
$\overline{\theta}$ = Average of the fluctuation of temperature
$\overline{\theta u_i}$ = Average turbulent heat flux in i direction
$\overline{u_i u_j}$ = Average turbulent stress
ε = Rate of dissipation of k
ε_θ = Rate of dissipation of $\overline{\theta^2}$
ζ = $-x(\partial T/\partial x)_{x=0}$

INTRODUCTION

The transport of energy in a convective medium is a combination of both thermal diffusion and enthalpy flow. So in order to visualize the true path of heat flow one has to take into account the flow of enthalpy at a particular point while taking into account the conductional energy flow. If the flow velocities are zero everywhere, then the enthalpy flow is also zero, so one only requires to plot the isotherms in order to get some idea of the path of heat flow, because the isotherms are then locally perpendicular to the direction of energy flow. However, to see the path of heat flow in a convective medium one has to define a heat function $H(x, y)$ such that the net flow of energy (thermal diffusion + enthalpy flow) across each H = constant line is zero, as has been defined by

0961–5539

Received September 1994
Revised June 1995

Kimura and Bejan[1]. The plot of such constant H line will be a proper representation of the flow of energy in a convective medium just as the stream lines represent the velocity field.

The first application of heatline for the visualization of convective heat transfer in a square cavity was made by Kimura and Bejan[1]. Thereafter the method has been adopted in the heat transfer literature and has been extended to several other convection configurations. The literature[2-7] describes the use of heatline and the concept of equivalent masslines in both cylindrical and rectangular co-ordinate systems. Dash and Chottopadhyay[8] have extended the use of heatline to spherical-polar co-ordinate systems and have shown the path of heat flow near a spherical droplet having radial mass efflux. The common feature of these applications of the heat function method is that they all belong to the class of laminar flow of pure fluids either in enclosures or in external flow. The use of heat function to visualize the energy flow in a turbulent flow field is yet to receive attention. Against this background the present work is directed towards the application of heat function to turbulent fluid flow and heat transfer near a vertical heated plate.

GOVERNING EQUATIONS

We shall first write down all the governing equations for mass, momentum and energy which describe the turbulent fluid flow and heat transfer near a vertical heated plate, before going on to develop the heat function for turbulent flow. For clarity, the continuity, momentum and the energy equations are written here in a tensorial form in a rectangular co-ordinate system. It should be noted here that all the terms of the Navier-Stokes equations are retained in the momentum and energy equations without making the boundary layer approximations. To describe the turbulence we made use of the low-Re-number-k-ε model along with the single point eddy diffusivity hypothesis to predict the turbulent shear as well as the normal stresses $\overline{u_i u_j}$. For predicting the turbulent heat flux $\overline{\theta u_i}$, in both the co-ordinate directions, an algebraic expression for $\overline{\theta u_i}$ is utilized according to Hanjalic and Vasic[9] which has been derived from its own transport equation. The variance of temperature $\overline{\theta^2}$, (square of the fluctuations of temperature) appearing in the expression of $\overline{\theta u_i}$ is solved directly from its own transport equation according to Hanjalic *et al.*[10] along with its rate of dissipation ε_θ. These sets of equations for $\overline{u_i u_j}$ and $\overline{\theta u_i}$ close the system of partial differential equations utilized to predict the required turbulence. The constants used in the model are shown in *Tables 1 and 2,* which are in accordance with Hanjalic *et al.*[10].

Continuity

$$\frac{\partial}{\partial x_i}(\rho U_i) = 0 \tag{1}$$

Momentum

$$\frac{D(\rho U_i)}{Dt} = -\frac{\partial p}{\partial x_i} + \frac{\partial}{\partial x_j}\left[\mu\left(\frac{\partial U_i}{\partial x_j} + \frac{\partial U_j}{\partial x_i}\right) - \overline{\rho u_i u_j}\right] - \rho\beta g_i (T - T_{ref}) \tag{2}$$

Table 1 Constants

σ_k	σ_ε	σ_θ	$\sigma_{\varepsilon\theta}$	C_1	C_2	C_3
1	1.3	1	1	1.44	1.92	1.44/0.8

Table 2 Constants

ϕ_θ	C^θ_1	C^θ_2	C^θ_3	C^θ_4	ζ	η
0 2	1.3	2.2	0.72	0.8	0.6	0.6

Energy

$$\frac{D(\rho T)}{Dt} = \frac{\partial}{\partial x_i}\left(\frac{\mu}{Pr}\frac{\partial T}{\partial x_i} - \rho\overline{\theta u_i}\right). \tag{3}$$

Turbulent kinetic energy

$$\frac{D(\rho k)}{Dt} = D_k + \rho P + \rho G - \rho\varepsilon. \tag{4}$$

Rate of dissipation of k

$$\frac{D(\rho\tilde{\varepsilon})}{Dt} = D_\varepsilon + C_1\rho P\frac{\tilde{\varepsilon}}{k} + C_3\rho G\frac{\tilde{\varepsilon}}{k} - C_2 f_\varepsilon\rho\frac{\tilde{\varepsilon}^2}{k} + E. \tag{5}$$

Variance of temperature

$$\frac{D(\rho\overline{\theta^2})}{Dt} = D_\theta + 2\rho P_\theta - 2\rho\varepsilon_\theta. \tag{6}$$

Rate of dissipation of $\overline{\theta^2}$

$$\frac{D(\rho\tilde{\varepsilon}_\theta)}{Dt} = D_{\varepsilon\theta} + C_1^\theta\rho P_\theta\frac{\tilde{\varepsilon}_\theta}{\overline{\theta^2}} + C_3^\theta\rho P\frac{\tilde{\varepsilon}_\theta}{k} - C_2^\theta\rho\frac{\tilde{\varepsilon}_\theta^2}{\overline{\theta^2}} - C_4^\theta f_\varepsilon\rho\frac{\tilde{\varepsilon}_\theta\tilde{\varepsilon}}{k} + E_\theta \tag{7}$$

where

$$\overline{\theta u_i} = -\phi_\theta\frac{k}{\varepsilon}\left(\overline{u_t u_j}\frac{\partial T}{\partial x_j} + \zeta\overline{\theta u_j}\frac{\partial U_i}{\partial x_j} + \eta\beta g_t\overline{\theta^2}\right)$$

$$\overline{u_t u_j} = \frac{2}{3}k\delta_{ij} - \nu_t\left(\frac{\partial U_i}{\partial x_j} + \frac{\partial U_j}{\partial x_i}\right), \nu_t = 0.09\, f_\mu\frac{k^2}{\tilde{\varepsilon}}$$

$$D_\phi = \frac{\partial}{\partial x_j}\left[(\mu + \frac{\mu_t}{\sigma_\phi})\frac{\partial\phi}{\partial x_j}\right], P = -\overline{u_t u_j}\frac{\partial U_i}{\partial x_j}, P_\theta = -\overline{\theta u_j}\frac{\partial T}{\partial x_j}$$

$$G = -\beta g_i\overline{\theta u_t}, E = 2\mu\nu_t\left(\frac{\partial^2 U_i}{\partial x_j\partial x_k}\right)^2, E_\theta = 2\rho\alpha\alpha_t\left(\frac{\partial^2 T}{\partial x_j\partial x_k}\right)^2$$

$$\tilde{\varepsilon} = \varepsilon - 2\nu\left(\frac{\partial\sqrt{k}}{\partial x_i}\right)^2, \tilde{\varepsilon}_\theta = \varepsilon_\theta - \alpha\left(\frac{\partial\sqrt{\overline{\theta^2}}}{\partial x_k}\right)^2$$

$$f_\mu = \exp\left[-3.4/(1+0.02Re_t)^2\right], \quad f_\varepsilon = 1 - 0.3\exp(-Re_t)^2, \quad Re_t = \frac{k^2}{\nu\varepsilon}.$$

DEVELOPMENT OF HEAT FUNCTION

The heat function is derived by satisfying the energy equation in the same way as the stream function is developed by satisfying the continuity equation. So to develop the heat function we write down here the expanded form of the energy equation (3) at steady state;

$$U\frac{\partial T}{\partial x} + V\frac{\partial T}{\partial y} = \frac{\partial}{\partial x}\left(\alpha\frac{\partial T}{\partial x} - \overline{\theta u}\right) + \frac{\partial}{\partial y}\left(\alpha\frac{\partial T}{\partial y} - \overline{\theta v}\right). \tag{8}$$

So we define

$$\frac{\partial H}{\partial y} = \rho C_p UT - \lambda \frac{\partial T}{\partial x} + \rho C_p \overline{\theta u} \tag{9}$$

net energy flux in x direction

$$-\frac{\partial H}{\partial x} = \rho C_p VT - \lambda \frac{\partial T}{\partial y} + \rho C_p \overline{\theta v} \tag{10}$$

net energy flux in y direction.

It can be seen here that equations (9) and (10) identically satisfy the energy equation (8). Hence, equations (9) and (10) stand for the proper description of heat function $H(x, y)$ for turbulent heat transfer in a convective medium in a cartesian co-ordinate system. It should be noted here that the flux equations in (9) and (10) look almost the same as those developed for laminar flow by Kimura and Bejan[1] with the only exception that these take into account the turbulent heat fluxes along with the enthalpy flow. In order to solve the heat function H, we proceed in the following way. Differentiate equation (9) with respect to y and equation (10) with respect to x and subtract the later from the former in order to get

$$\frac{\partial^2 H}{\partial x^2} + \frac{\partial^2 H}{\partial y^2} = \rho C_p \left(\frac{\partial}{\partial y}(UT + \overline{\theta u}) - \frac{\partial}{\partial x}(VT + \overline{\theta v}) \right). \tag{11}$$

So equation (11) is the proper partial differential equation for $H(x, y)$ which should be solved in the flow field to predict the value of H in the entire domain. The right hand side of equation (11) is known from the solution of the flow and temperature field. The turbulent heat fluxes $\overline{\theta u}$ and $\overline{\theta v}$ are also known in the process of solving the flow field. Now equation (11) can be solved with a proper set of boundary conditions for H, which are defined from the definition of flux (equations 9 and 10) and are shown in *Figure 1*.

Boundary conditions

The boundary conditions used for the equations (2-7) and (11) are shown pictorially in *Figure 1*. The line having the hatches represents here the heated vertical wall of 10 metres. The far stream boundary is kept at a distance of 3.5 metres from it where the U component of velocity is determined from the pressure boundary conditions (the boundary pressure is kept at zero) and the V component of velocity from the Euler equation. For all other variables at the far stream boundary a zero gradient condition is used. At the inlet the temperature is kept at $T\infty$ and the velocities are kept at zero along with the turbulent kinetic energy k, ε, $\overline{\theta^2}$ and ε_θ. At the outlet boundary zero gradient conditions for all variables are used. The boundary conditions for H follow from the definition of H defined in equations (9 and 10). At the wall $\partial H/\partial x$ is zero because V and $\overline{\theta v}$ are zero there and $\partial T/\partial y$ vanishes because the wall temperature is constant. At the far stream boundary also the same conditions prevail, hence $\partial H/\partial x$ is zero there. At the inlet we specify U to be zero, T = $T\infty$ and also $\overline{\theta u}$ is zero. So $\partial H/\partial y$ becomes identically zero excepting on the very first grid near the wall where $\partial H/\partial y$ is equal to $-\lambda \partial T/\partial x$. On the outlet boundary simply equation (9) is used to determine the value of H. At the leading edge of the plate the value of H is identically zero and at the top edge,

$$H = \int_0^{10} -\lambda \frac{\partial T}{\partial x}\, dy$$

which represents the total heat going away from the wall.

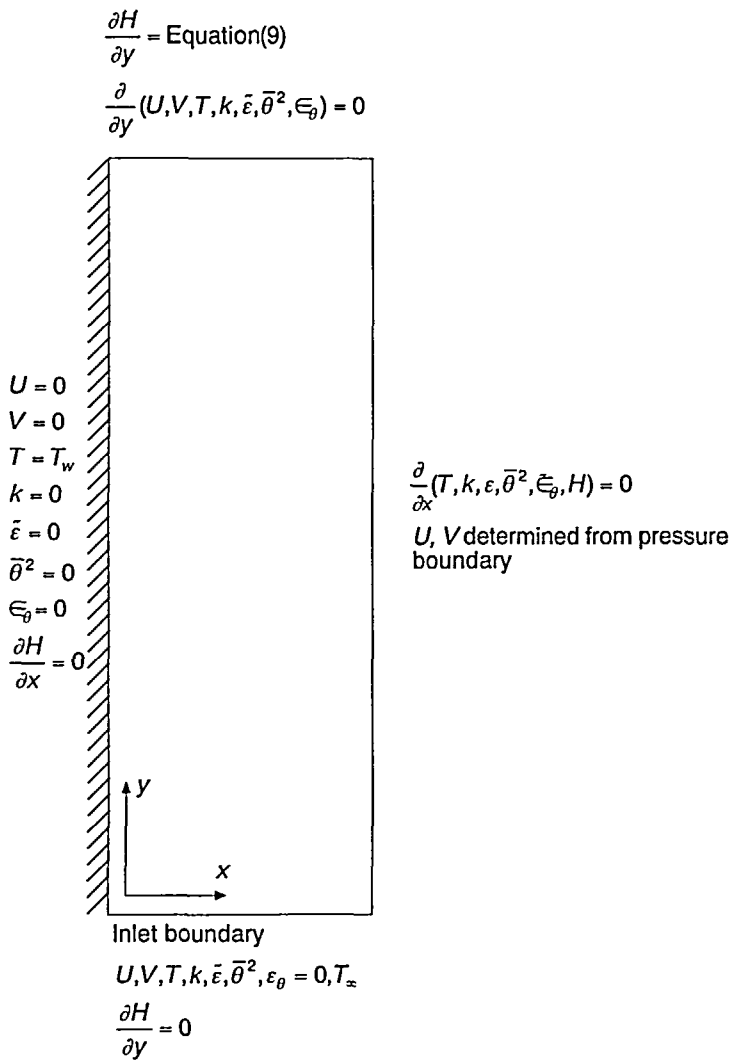

Figure 1 Boundary conditions used for the heated vertical plate

METHOD OF SOLUTION

The equations (2) to (7) with the help of the continuity equation (1) were solved numerically by means of a control volume numerical code based on the TEACH algorithm. The use of non-uniform staggered grid was made to compute the field properties like U, V, p, T, k, ε etc. A line by line iterative method with the tri-diagonal matrix algorithm (TDMA) was used to solve the velocity field, while the pressure field was solved with the SIMPLE algorithm by employing the Stone's strongly implicit procedure (SIP). Other variables like T, k, ε, $\overline{\theta^2}$ and ε_θ were solved with the help of the SIP algorithm. A strongly non-uniform grid was used near the wall to take into account the low Re number effects. The equations were interatively solved on a false time step marching having a time step of 0.00002 initially and subsequently increased slowly to 0.0001 per iteration. To initiate the turbulence a very low value of k 5 × 10^{-4} and ε 10^{-4} was taken as a guess in the flow field so that the turbulent Reynolds number was typically 100 everywhere. This guess

value of k and ε was found sufficient to initiate turbulence and no other triggering mechanism was required to get the transition. Almost 50,000 time steps were required to attain convergence. The convergence criteria were based on the fact that the sum of absolute residuals in each individual equation should be less than 10^{-4}. The computational domain had a size of 10 × 3.5m which was discretized by 81 × 71 control volumes. This size of the control volume was found adequate to describe the field properties to the accuracy of experimental results. The above computation was carried out for air near a heated vertical flat plate, where the plate temperature was kept at 60°C and the far stream ambient temperature being at 20°C.

After a converged solution was obtained an attempt was made to solve for the heat function described by equation (11). The solution was obtained on the non-uniform grid by employing a finite difference form of equation (11) which was solved by a Gauss-Siedel successive over relaxation method. Only 500 iterations were sufficient to bring convergence, where the same convergence criteria were used as above.

RESULTS AND DISCUSSION

As the aim of the present work is to develop a heat function and utilize the same in order to visualize the energy flux in a turbulent convective medium, we will restrict our discussion to only some aspects of the flow field which are important from the viewpoint of heat function. To compute the heat function from equation (11) it is necessary to compute very accurately the gradient of the temperature near the vertical plate, because this gradient is directly integrated over the height of the plate to arrive at the total heat going out from the plate, which is directly put as a boundary value for H at the top edge of the plate. Moreover, the value of H found at the first grid near the plate is directly assigned on to the plate because $\partial H/\partial x$ is zero on the plate. So from this viewpoint, the near wall flow and temperature field play a much more important role in deciding the value of H near the wall compared to other variables like turbulent heat flux $\overline{\theta u}$ and $\overline{\theta v}$, which are practically negligible very near to the wall along with its derivatives. In order to ascertain the temperature gradient near the wall we have computed the local Nusselt number on the plate and have compared that with the experimentals of the Tsuji and Nagano[11] in *Figure 2*. The agreement of the local Nusselt number with that of the experiment is very good and it can also be seen that the transition from laminar to turbulence is also predicted almost accurately. *Figure 3* shows the

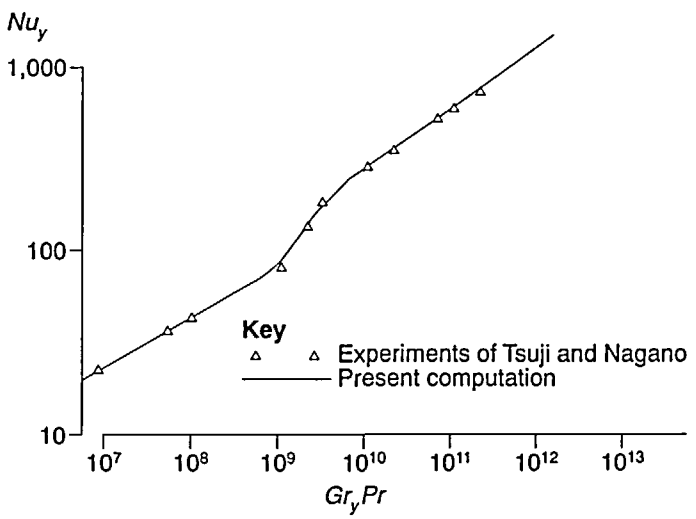

Figure 2 Variation of local Nusselt number along the vertical heated plate

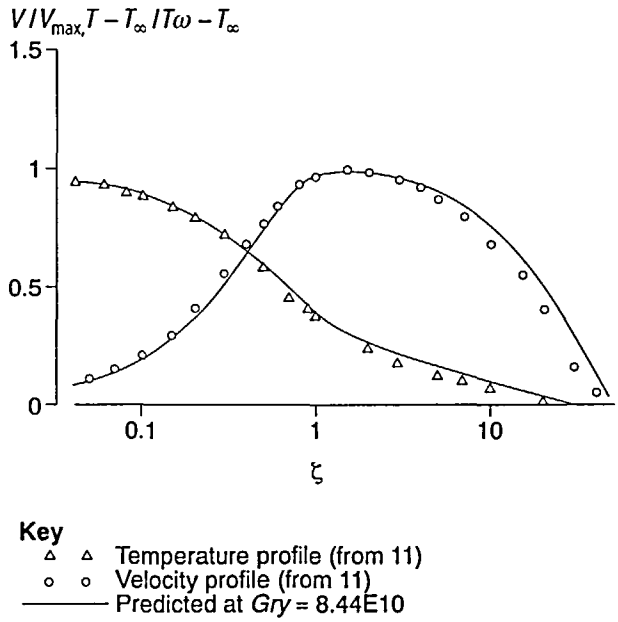

Figure 3 Comparison of the velocity and temperature field with that of the experiment

agreement of the velocity and temperature field with that of the experiment of Tsuji and Nagano[11] at a *Gr* number of 8.4×10^{10}.

In *Figure 4* the flow field and the temperature field in the entire domain is shown in terms of stream lines and isotherms. It can be observed that there is entrainment from the free stream boundary towards the heated plate and this entrainment of the surrounding fluid is solely responsible for maintaining the increased mass flux near the plate with the increase in plate height. The isotherm plot in *Figure 4b* shows the development of the turbulent thermal boundary layer near the heated vertical plate. It can be seen that the thickness of the thermal boundary layer at the top edge of the plate is around 20% of the width of the computational domain. This means in a large part of the domain, excepting the near wall region, conduction heat transfer is virtually negligible. However, the plot of the isotherm here does not give any impression about the direction of the energy flow in the convective medium.

Figure 5a shows the energy flux in terms of heatline in the entire flow field. As is seen, there is flux of energy coming from the free stream towards the plate but they do not feed heat to the plate because they are really not meeting the plate. As the plate is hot compared to the free stream ambient so the plate gives out energy to the ambient which is shown in a blown up view in *Figure 5b*. The heatline in *Figure 5a* looks almost the same as that of the stream lines away from the plate. This is because the energy flux away from the plate is mainly due to the enthalpy flow. Transportation of energy due to conduction is virtually zero as has been explained above. As there is entrainment flow from the free stream so there is also enthalpy from the free stream, and this is the reason why the heatlines look like the stream lines away from the heated plate.

What happens near the plate is shown in *Figure 5b*. This figure is obtained by stretching *Figure 5a* in the *x* direction so as to see a very close view near the plate. Heatlines *a-d* having positive values, start from the heated wall and go up, showing the removal of energy from the plate and thereafter being lifted up by the nearby convection field towards the outlet side on the top edge of the plate. Here the heatlines *a-d* are actually perpendicular to the wall because of the zero gradient conditions imposed on them. However, it is difficult to see this phenomenon here because the grid density near the wall is very high; the first grid is about 0.2mm from the wall, and the

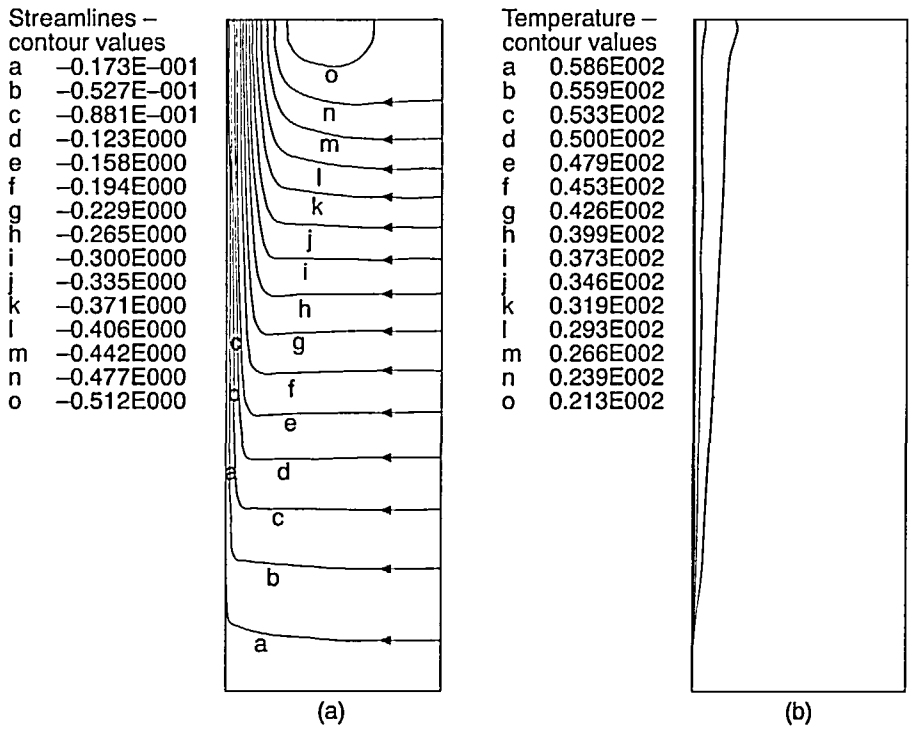

Figure 4 A plot of streamlines and isotherms in the turbulent flow field near a heated vertical plate

magnification used in *Figure 5b* is not great enough to resolve this phenomenon. The value of the heatline increases from *a* to *d* in the positive *y* direction. This means that $\partial H/\partial y$ is positive and hence the energy flux is in the positive *x* direction, implying the fact that energy is being removed from the hot plate. If there were no convective field around the plate then the heatlines *a-d* would have moved parallel to the *x* axis towards the free stream (implying a case of pure conduction). Because of the presence of the strong buoyant velocity near the plate, the heatlines *a-d*, although they start normally from the wall, immediately go up in the *y* direction in order to account for the vertical energy flux present there. The heatlines *e* to *j* are increasing negative values in the positive *y* direction. This means that $\partial H/\partial y$ is negative and the energy flux is in the negative *x* direction, implying the fact that energy is being carried in from the free stream ambient. Such visualization of energy flow in the buoyancy-driven turbulent field is only possible because of the construction of the heat function, equation (11). Otherwise it is impossible to see this phenomenon from a plot of the isotherms in *Figure 4b*.

CONCLUSIONS

The use of a four equation low-*Re*-*k*-ε algebraic flux model is made to predict the characteristics of a turbulent natural convection near a vertical heated plate. In particular use of an algebraic flux model for the turbulent heat transport is made in order to take into account the details of the turbulent heat flux $\overline{\theta u}$ and $\overline{\theta v}$. Then the heat function was developed for the turbulent fluid flow and was utilized to show the true path of heat flow in a buoyancy-driven turbulent flow field near a vertical heated plate. Without the construction of this heat function (equation (11)) it would have been impossible to see the fact that energy flows from the free stream ambient towards a heated plate even when the plate is being cooled by the surrounding convection current.

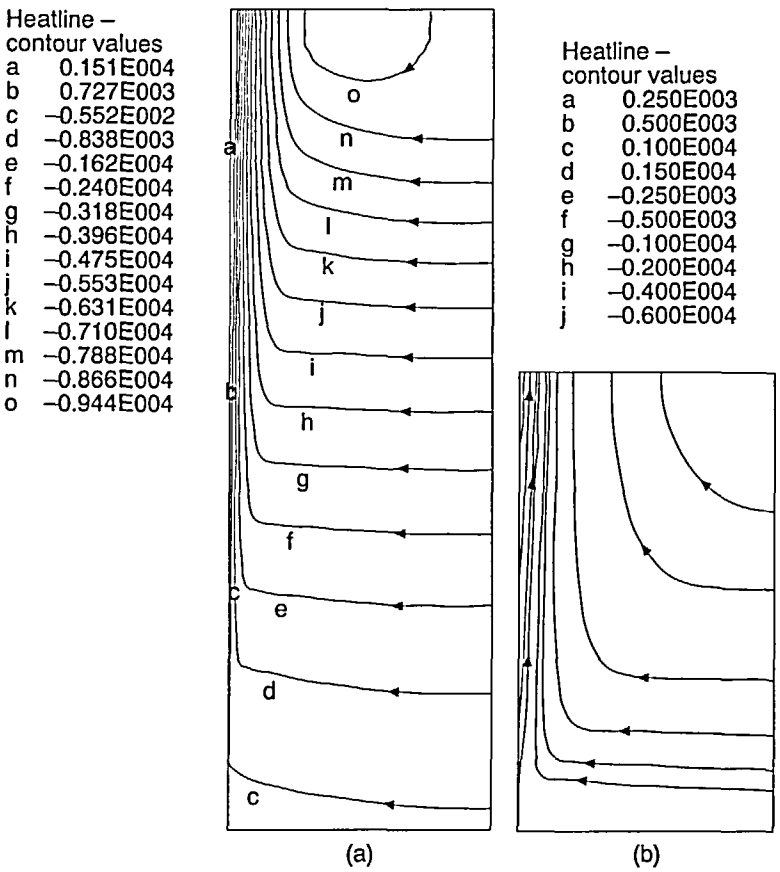

Figure 5 A plot of heatline in the turbulent flow field near a heated vertical plate

ACKNOWLEDGEMENTS

The author gratefully acknowledges the financial support given to him by the Alexander von Humboldt Foundation to carry out his research work at the Friedrich Alexander University of Germany for which the present work became possible. The author also expresses his thankfulness to S. Kenjeres for his valuable suggestions in carrying out the computation.

REFERENCES

1 Kimura, S. and Bejan, A., The heatline visualization convective heat transfer, *J. Heat Transfer,* **105,** 916-919 (1983)
2 Morega, Ai. M. and Bejan, A., Heatline visualization of forced convection in poros media, *Int. J. Heat and Fluid Flow,* **15,** 40-47 (1993)
3 Aggarwal, S.K. and Manhapra, A., Use of heatlines for unsteady buoyancy driven flow in a cylindrical enclosure, *J. Heat Transfer,* **111,** 576-578 (1989)
4 Bello-Ochende, F.L., Analysis of heat transfer by free convection in tilted rectangular cavities using the energy analogue of the stream function, *Int. J. Mech. Eng. Education,* **15,** 91-98 (1987)
5 Bello-Ochende, F.L., A heat function formulation for thermal convection in a square cavity, *Int. Comm. Heat Mass Transfer,* **15,** 193-202 (1988)
6 Littlefield, D. and Desai, P., Buoyant laminar convection in a vertical cylindrical annulus, *J. Heat Transfer,* **108,** 814-821 (1986)

7 Trevisan, O.V. and Bejan, A., Combined heat and mass transfer by natural convection in a vertical enclosure, *J. Heat Transfer,* **109,** 104-109 (1987)
8 Dash, S.K. and Chattopadhyay, H., Numerical visualization of convective heat transfer from a sphere – with and without radial mass efflux, *Int. J. Num. Methods Heat and Fluid Flow,* **4** (1994)
9 Hanjalic, K. and Vasic, S., Computation of turbulent natural convection in rectangular enclosures with an algebraic flux model, *Int J. Heat Mass Transfer,* **36,** 3603-3624 (1993)
10 Hanjalic, K., Kenjeres, S. and Durst, F., Numerical study of natural convection in partitioned 2-dimensional enclosures at transitional Rayleigh numbers, *10th Int. Heat Mass Transfer Conf.* (1994)
11 Tsuji, T. and Nagano, Y., Characteristics of a turbulent natural convection boundary layer along the vertical flat plate, *Int. J. Heat Mass Transfer,* **31,** 1723-1734 (1988)